THE MOTOR SYSTEM: NERVE REGENERATION AND NEURAL PROSTHETICS

Lesions in the peripheral nervous system in humans can lead to several disabling effects in sensory and motor functions because the primary information carrier, the propagating action potential, can no longer travel from sensory organs to the brain (afferent information, sensory nerve fibers) or from the brain to muscles (efferent information, motoneurons). In many cases, peripheral nerves may "repair themselves" (regeneration), provided that the source of the lesion (for example, pressure on the nerve) is removed soon enough or that adequate surgical measures are taken in due time in order to bring nerve stumps together or to transplant nerve sections to bridge a large gap. During the healing process, nerve fibers will first degenerate and then regenerate all the way, from the spinal cord toward the periphery, reusing the old channels of myelin sheaths and connective tissue. The nerve regenerates with a typical speed of 1 mm per day.

However, this ability to regenerate more or less autonomously is a property of peripheral nerves only. The central nerve fibers of the spinal cord cannot be induced to regenerate, although extensive research tries to bring this about by manipulating the biochemical environment of the fibers, offering proteins such as neural growth factors or semaphor proteins and other agents that may stimulate nerve growth.

If a person has a central neural lesion but no harm to the peripheral nerves—for example, in paraplegic individuals (with neural interruptions in the spinal cord)—the peripheral nerves may be stimulated artificially by short electric pulses, which evoke propagating action potentials toward the paralyzed muscles and restore force.

Crude restoration of basic motor function has been achieved in laboratory settings using surface electrodes or implanted wires, to control on the order of ten muscles, in a

more or less on–off way of operation, which causes fast fatiguing of the muscle. More complicated everyday functions will require independent control of a large number of nerve fibers/fascicles/muscle units, which allows finely tuned motion and does not cause fatigue. Besides highly developed, multisite contacting technology, sophisticated closed-loop control is necessary for those functions, as well as the help of mechanical and other nonelectrical prosthetic aids. Research on all aspects is in full swing but will take many years to reach the clinical application level.

Nonmotor Systems

Artificial electric stimulation is used to stimulate the auditory nerve in cases of profound hair cell damage in the cochlea. This application is widespread clinically. Other applications are bladder stimulation of the nerves of the urinary system, diaphragm pacing, cardiac pacing. In these cases, the number of electrodes is only one or relatively modest.

MODELING OF ELECTRICAL STIMULATION OF FIBERS IN PERIPHERAL NERVE

Peripheral nerve consists of (up to thousands of) nerve fibers, or axons, with diameters ranging from a few to tens of micrometers. Nerves may contain subbundles, called fascicles, with a typical diameter of 0.5 mm. Motor fibers have a myelin sheath wrapped around them, to speed propagation of the action potential. At regular intervals λ the myelin sheath is interrupted over a few micrometers, at the so-called nodes of Ranvier. These are the sites where membrane channels exchange ions into and out of the membrane, to keep the action potential traveling. The ratio of internode distance to fiber diameter is approximately 100 : 1.

A negative-going extracellular current pulse close to a node may trigger the action potential artificially. This is the basis of artificial electrical stimulation.

Modeling is usually done in two stages, with a nerve fiber excitation model and a volume conductor model.

The Nerve Fiber

First, the response of a nerve fiber to an electrical field is modeled (1,2). For this, the approximate activating function may be used, in which a fiber is considered over a length of three nodes only, modeled by two sections of a passive *RC* network (Fig. 1). The nerve becomes active when the second-order difference f of external node potentials V_e of a central node and its two neighbors exceeds a threshold (about 20 mV). As the exact node positions are unknown and f for a given diameter class of fibers only depends on the internode distance λ, activating functions are calculated for each position x,y,z and $x,y,z \pm \lambda$ in the fascicle, for each electrode. Thus

$$\begin{aligned} f &= V_{e,n-1} - 2V_{e,n} + V_{e,n+1} \\ &= V_e(x, y, z-\lambda) - 2V_e(x, y, z) + V_e(x, y, z+\lambda) \end{aligned} \tag{1}$$

If an electrode is sufficiently close to a node of Ranvier, compared to λ, the two terms $V_{e,n-1}$ and $V_{e,n+1}$ may be set to zero. This is the local approach.

The activating function sets the external potential condition but does not take into account ionic currents through the membrane ion channels, which can be modeled by the famous Hodgkin–Huxley equations and their refined forms. Because of this, the activating function approach is only valid for short rectangular stimulus current pulses, in the range of 10 μs to 100 μs duration. Also, the well-known relationship at the threshold of stimulation between amplitude and duration of the stimulus (strength-duration threshold curve) is not contained in the activating function.

The effect of pulse duration has been taken into account recently by Warman et al. (3). Nagarajan and Durand (4), Grill and Mortimer (5), and others. It was demonstrated that it may be a tool to influence spatial selectivity of stimulation.

The metal electrode itself, with its interface to the fluid environment (Helmholtz layer, Warburg impedance, Faradaic current), is not dealt with here but is an important part of the stimulation system.

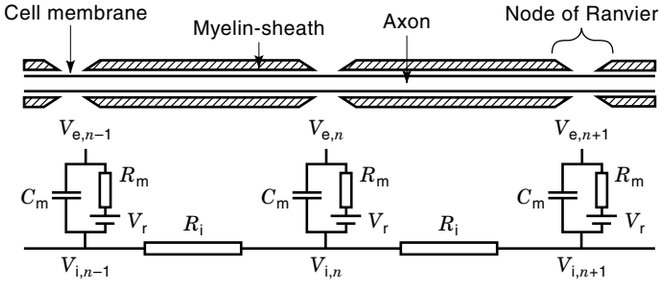

Figure 1. The electric network equivalent of a myelinated fiber. V_r is the membrane rest potential. $V_{e,n}$ is the extracellular potential at node n. $V_{i,n}$ is the intracellular potential at node n. R_i is the intracellular resistance. C_m and R_m are membrane capacitance and resistance.

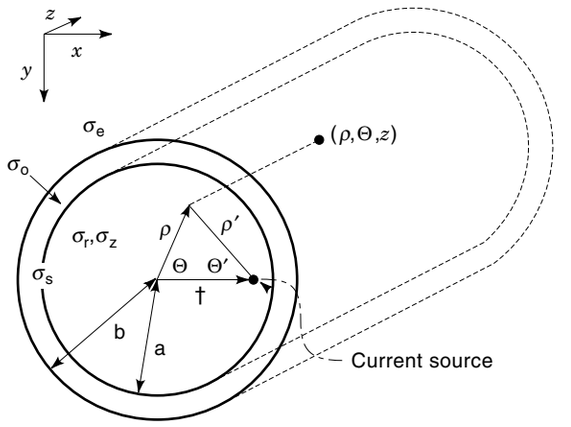

Figure 2. The volume conduction model of the nerve and its surroundings. Longitudinal and radial conductivity inside the fascicle are σ_z and σ_r, respectively. Perineural sheath conductivity is σ_s, epineural conductivity σ_o, and extraneural conductivity σ_e.

The Volume Conductor

Second, the potentials $V_{e,n}$, generated by currents from stimulating electrode configurations, must be calculated at the node positions of all fibers and represented as equipotential contours, or equiactivation function contours (6).

Figure 2 shows the volume conductor model of a cylindrical nerve or fascicle. The fascicle is idealized as an electrically homogeneous and infinitely long extending cylinder with a ra-

dial conductivity σ_r and a longitudinal conductivity σ_z. The cylinder is surrounded by a layer that represents the thin perineurium, with a sheath conductivity σ_s. The next layer is the perineurium, with conductivity σ_o. At the outside of the fascicle the medium is infinitely homogeneous and isotropic with conductivity σ_e.

Stimulation electrodes are idealized as point current sources and may be positioned anywhere in the fascicle. Using the cylinder symmetry, an analytical expression for the potentials can be derived. The potential V_e for an electrode at $(r,0,0)$—injecting current I—consists of the sum of a source term V_e^s

$$V_e^s(x, y, z) = \frac{I}{4\pi\sqrt{\sigma_r\sigma_z}\sqrt{(x-r)^2 + y^2 + z^2\sigma_r/\sigma_z}} \qquad (2)$$

and a boundary term V_e^b, which is an expansion of Bessel functions. Similarly, $V_e^s(x,y,z+\lambda)$ follow from (Eq. 2).

Electrode configurations may be monopolar, bipolar, tripolar, and so on. Combinations of anodes and cathodes may yield some field-steering capability, although at the expense of higher stimulus currents (6,7).

While the cylindrical idealization of the nerve or fascicle permits the analytical solution of Laplace's equation, as summarized previously, the more general case of a nerve volume conductor with many irregular, inhomogeneous, anisotropic fascicular cross sections inside asks for finite-difference modeling of the tissue (8,9).

SELECTIVITY OF STIMULATION AND EFFICIENCY OF A STIMULATION DEVICE

At low current, an electrode can stimulate one fiber if its position is close to that fiber, compared to other fibers. Increase of current will expand the stimulation volume, thus including more and more fibers.

The ultimate selectivity would be reached if each fiber would have its own electrode. This would require, however both a blueprint of positions of fibers in the nerve so that electrodes could be positioned close to a node of Ranvier, and enough electrodes. In practice, no blueprint is available, and microfabrication has technological limits. Therefore, with a limited number of electrodes, placed optimally (in a statistical sense), it is important to consider and test how selective stimulation can be.

In this respect one has to measure the extent to which each electrode controls as few fibers as possible at low current, before potential fields start to overlap with those of other electrodes, with increase of current. Greater overlap means lower selectivity.

From another point of view, one might define the efficiency of a multielectrode device: the number of distinct fibers that can be contacted, divided by the total number of electrodes. Greater overlap means reduced efficiency.

Fiber selectivity has been addressed in Rutten et al. (10), among others. It was concluded, on statistical grounds and by overlap experiments, that an electrode separation of 128 μm was optimal for a rat peroneal nerve fascicle with 350 alpha motor fibers.

Limited force recruitment experiments with a 2 D 24-electrode array (electrode separation 120 μm) (11) yielded that 10 distinct threshold forces could be evoked (efficiency is 10/24 = 42%).

PERIPHERAL NERVE FIBER RECORDING: MODELING AND SELECTIVITY

The forward control of muscle by artificial stimulation might gain importance when this control is supplemented by selective feedback information from nerve fibers attached to sensors such as muscle spindles, tendon organs, and cutaneous sensors. This asks for insight into selective recording with multielectrodes.

The same type of calculation previously made for the case of selective stimulation of nerve fibers in rat peroneal nerve (isotropic conductor, local approach) (10) could be applied, by reciprocity, to the case where the device is used to sense natural activity from afferent fibers. These calculations would, for example, lead to a (statistically optimal) electrode interdistance of 143 μm, for the case that there are 250 type I afferent fibers in rat peroneal nerve.

However, while an action potential can be triggered by activation of one node of Ranvier only (stimulation), propagation of an action potential requires about 20 active nodes (recording). So it is not allowed to replace the electrode (stimulation) by one node of Ranvier (recording).

Another difference is that nerve fibers will almost always fire as ensembles. Regarding selectivity, when two (not overlapping in time) action potentials (or ap trains) are sensed by one electrode, the trains can be detected separately when the selectivity ratio S of their amplitudes V_1 and V_2 exceeds a certain threshold (i.e., when $S > S$th; for example, $S > 1.1$, or $S > 2$) (compare this to the signal-to-noise ratio; 1.1 means barely visible, 2 is better).

Quantitative insight in this selectivity ratio S as a function of spatial and conductivity parameters may be obtained by the combined use of an electrode lead field model (using the volume conduction model as outlined previously) and a probability model for the positions of active fibers (12). Figure 3 shows a dramatic decrease in the ability to discriminate two trains when the nerve is insulated from its surrounding tis-

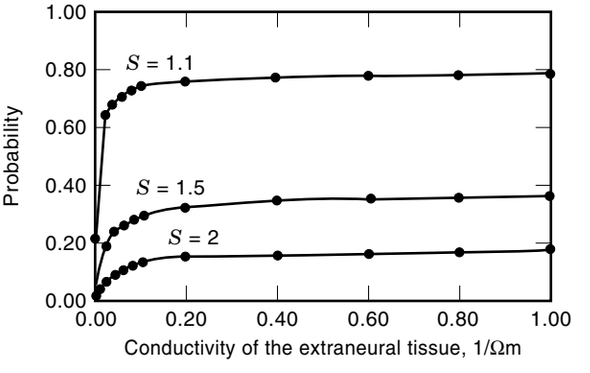

Figure 3. The probability P that the measured action potentials from the two fibers, which are nearest to a central monopolar electrode, have an amplitude ratio $S > S_{threshold}$ for three thresholds 1.1, 1.5, or 2, as a function of the conductivity of the extraneural tissue. The nerve has 40 active fibers (20 nodes each). (From Ref. 12.)

sue (i.e., for zero extraneural conductivity), illustrating the importance of a natural wet surrounding of the nerve.

MICROFABRICATED LINEAR, 2-D, AND 3-D MULTIELECTRODES

Silicon and Silicon-Glass Arrays

Silicon-based microprobe fabrication has been a major and outstanding activity of the Center for Integrated Sensors and Circuits at the University of Michigan and has led to a large number of single-shaft, multishaft, and 3-D stacked microelectrode arrays, a number of these being supplied with onboard microelectronics (13–22). Fabrication was supported by design studies (23), strength characterization (24), and development of interconnection technology (25,26). Groups in Utah and Twente tried to fabricate brush or needle-bed 2-D/3-D multielectrodes in silicon or silicon/glass technology, for cortical and nerve applications, with about 100 electrodes. As anisotropic silicon etching cannot (yet) perform up to the aspect ratios needed for long, slim needles (a 20 μm diameter, 500 μm long needle has an aspect ratio of 25); the first step to obtain a brush structure from a solid piece of silicon is a sawing procedure (12,27,28).

Silicon/glass technology has the advantage of high aspect ratios, sufficient lengths of needles, and different lengths of needles in the same device. The disadvantages are the 3-D nature of many of the process steps, the large number of steps, and the difficulty of their integration (12).

The 3-D cortical multielectrode array, using microassemblies of 2-D planar probes, of the Michigan group (20) is a good example of a hybrid fabrication solution: stacking of multishaft/multisite flat devices, combining many advantages.

Silicon-LIGA Arrays

An alternative, batch-oriented, and larger-scale way to fabricate multielectrode needle-shaped devices is to combine silicon technology with the LIGA technique (Lithographie, Galvano Abformung) (29). Briefly, in the silicon/LIGA process nickel needles are grown from a combined seed/interconnection layer through narrow channels in 200 μm PMMA (polymethylmethacrylate). After removal of PMMA and etching of the seed layer, the electrode needles stand completely electrically separated and are connected individually to the leads in the interconnection layer.

In this way, Bielen succeeded at the IMM (Institute fur Microtechnologie in Mainz, Germany) in fabricating a 2-D multielectrode of 4 $\times$ 32 needle electrodes, with square as well as round columns or needles. The electrodes have a thickness as low as 15 μm and an ultimate height of 220 μm (11).

Silicon/LIGA technology reduces the number of steps but has as a disadvantage the need for synchrotron radiation facilities. Also, the present limit of the electroplating process to 220 μm long nickel needles has to be extended to a needle length of about 500 μm for useful neuroprosthetic and cortical applications.

A review of electrode technology and its perspectives can be found in Mortimer et al. (30). An interesting, nonsilicon approach to contact fibers intrafascicularly is the use of teth-

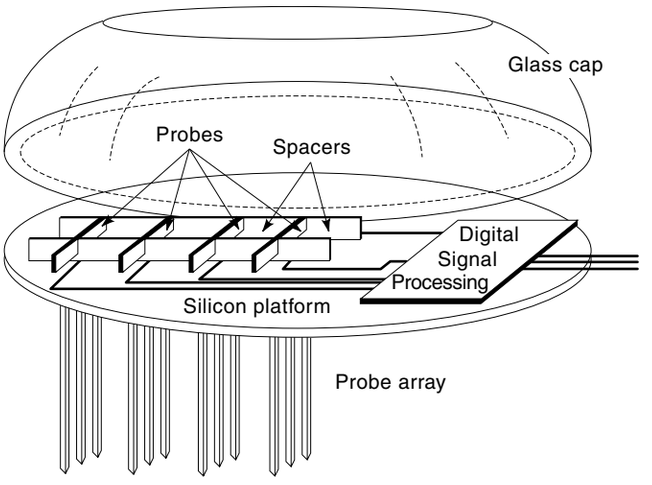

Figure 4. (a) Overall diagram of a surface-mounted 3-D recording array. Several multishank 2-D probes are inserted through the platform and held in place with micromachined spacer bars. (From Ref. 20, their Fig. 1.) (b) Scanning electron microscope (SEM) photographs of a 3-D 4 $\times$ 4-shank microelectrode array. The shanks on the same probe are spaced on 150 μm centers and are 40 μm wide. The probes are 120 μm apart in the platform. (From Ref. 20, their Fig. 2, bottom.)

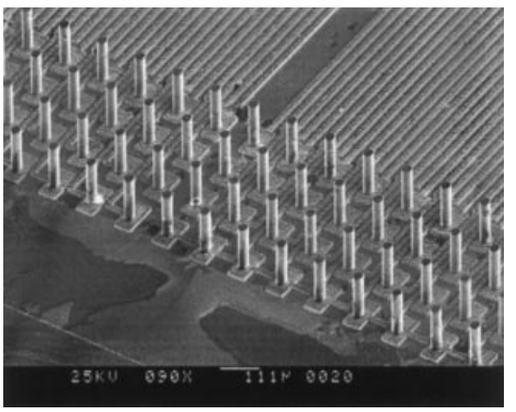

Figure 5. SEM photograph of silicon-nickel-LIGA array. Array with 150 μm tall, 20 μm diameter nickel needles, realized with aligned X-ray lithography and galvanic growing (LIGA) on silicon substrate with 8 μm Cu interconnection wiring. Interdistance between columns is 120 μm. (From Ref. 11.)

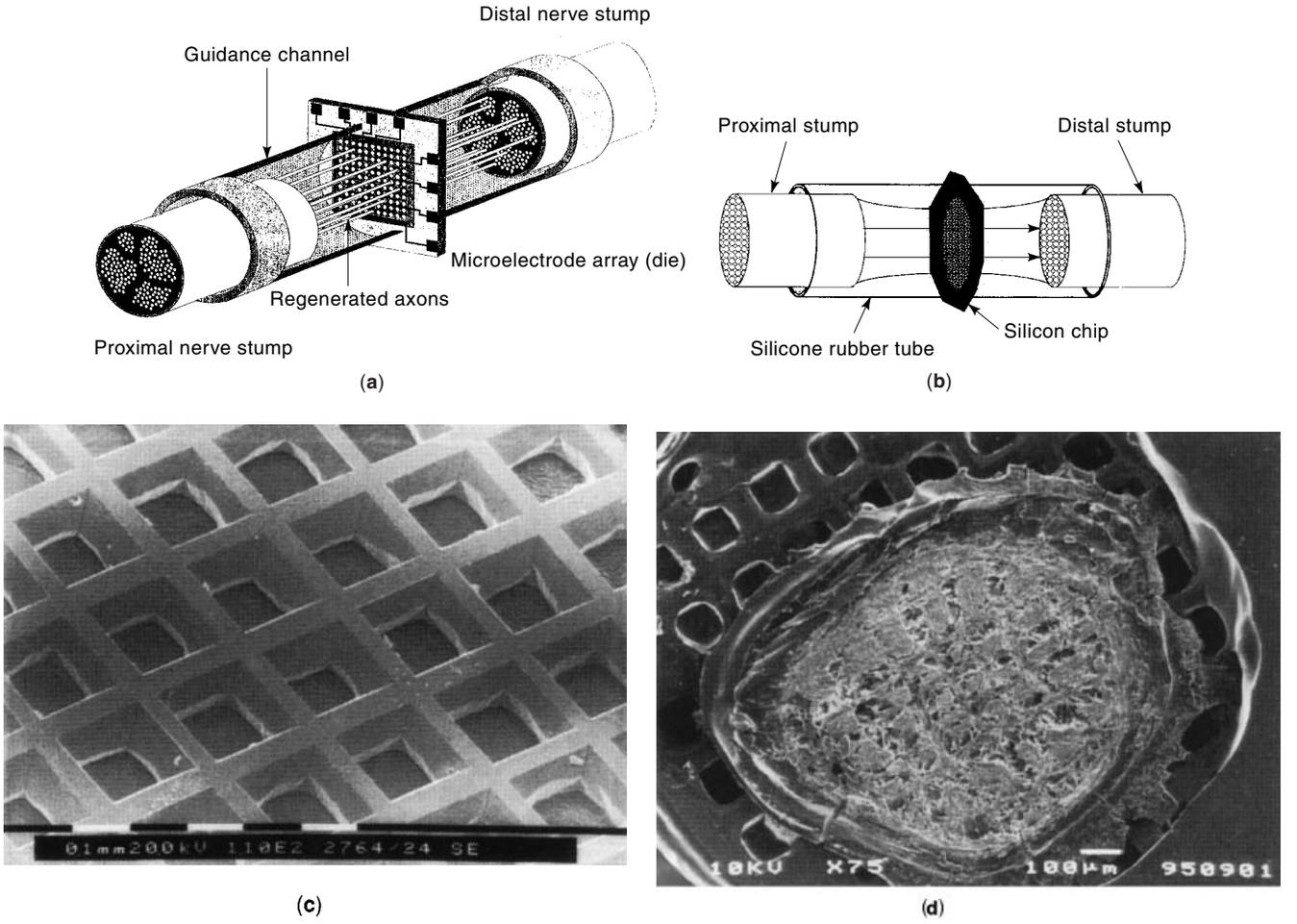

Figure 6. (a) Schematic representation of an intelligent neural interface implanted into an intersected nerve. (From Ref. 43, their Fig. 1.) (b) Schematic drawing of the silicone chamber model with the inserted silicon chip bridging a 4 mm gap between the proximal and distal stumps of a transected rat sciatic nerve (From Ref. 42, their Fig. 3.) (c) SEM photograph view of a fabricated chip with 100 μm diameter holes. (From Ref. 42, their Fig. 2.) (d) SEM photograph of nerve tissue sections distal to a chip with hole diameters of 100 μm after 16 weeks of regeneration. Shown is a minifascicular pattern on the distal surface of the chip. The regenerated nerve structure has a smaller diameter than that of the perforated area of the chip. The circumferential perineurial-like cell layer is clearly visible. (From Ref. 42, their Fig. 5, top.)

ered Pt microwires (25 μm diameter), developed by Horch and colleagues (31–38).

OTHER TYPES OF INTERFACES BETWEEN ELECTRODES AND NERVE TISSUE

Thus far, insertion of multielectrodes into peripheral nerve has been considered. As stated, one problem in this approach is that electrodes may have no target (fiber) close enough to be exclusive to one electrode (overlap problem). This lowers the efficiency of a multielectrode. Other ways to interface electrodes and nerve tissue are the regeneration of nerve through so-called sieves and the culturing of nerve cells on patterned multielectrode substrates. Both involve growth of nerve fibers or neurites. If successful, the principal advantage of such devices would be that each electrode has close contact to specific nerve fibers, reducing the overlap problem and increasing electrode efficiency.

Especially in neural culturing on planar substrates, a good understanding of the neuron–electrode interface is of primary concern and can directly be studied.

Both types of interfaces will be dealt with in subsequent sections.

REGENERATION SIEVE MICRO ELECTRODE ARRAYS

Another way of interfacing nerves to electrodes is the use of a 2-D (planar) sieve put in between the two cut end of a nerve. The silicon sieve permits nerve fibers to regenerate through metallized hole (or slit) electrodes in the sieve (39–43). The main advantage of this method is that microfabrication of flat devices is easier than that of 3-D devices. Another advantage

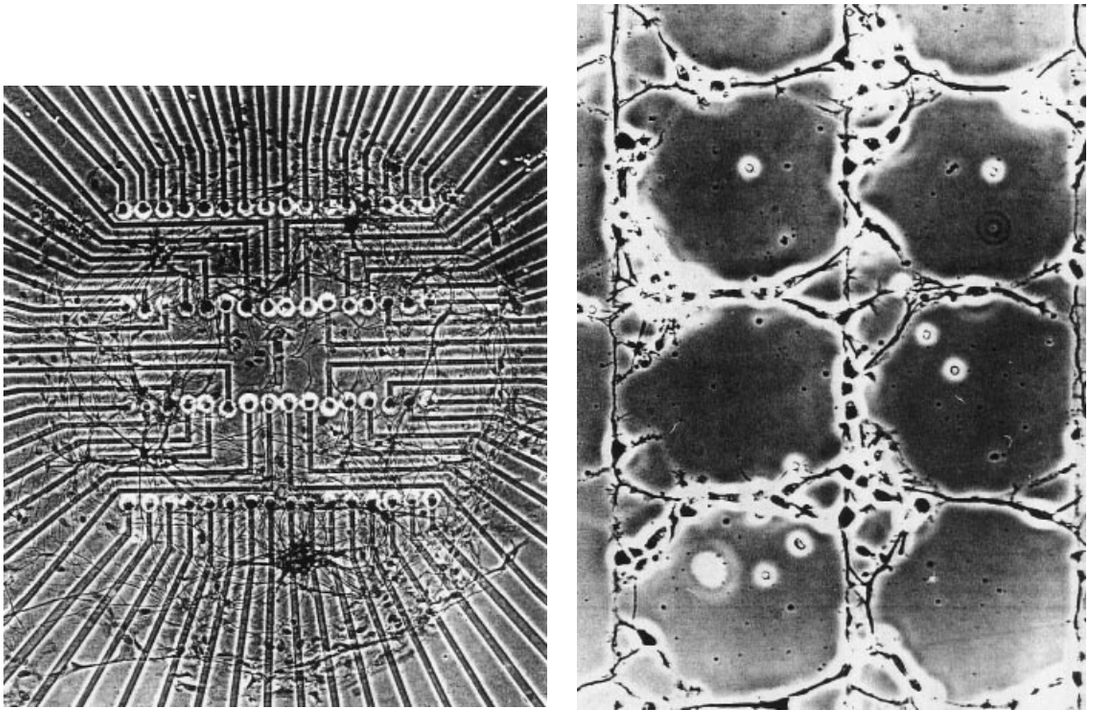

(a) (b)

Figure 7. (a) Low-density neuronal monolayer culture composed of 76 neurons growing over a matrix of 64 electrodes. The recording craters are spaced 40 μm laterally and 200 μm between rows. The transparent indium tin oxide conductors are 10 μm wide. Tissue is mouse spinal cord; culture age is 27 days in vitro; histology is Loots-modified Bodian stain. (From Ref. 60, their Fig. 2, p. 284.) (b) Cultured hippocampal neurons on patterned self-assembled monolayers. A hybrid substrate pattern of trimethyloxysilyl propyldiethylenetriamine (DETA) and perfluorated alkylsilane (13F) showing selective adhesion and excellent retention of the neurites to the DETA regions of the pattern. (From Ref. 6, their Fig. 4, p. 18.)

is that, once the nerve has been regenerated, the device is fixed firmly to the nerve. However, since the flats are typically only 10 μm thick, there is a limited chance that nodes of Ranvier will be close to an electrode (typical internode spacing of a 10 μm fiber is 1 mm), thereby limiting the selectivity of stimulation/recording. Also, nerve fibers tend to grow through holes not as single fibers, but as a group (fasciculation), thereby reducing the possibility of selective stimulation. Zhao et al. (42) report that only when nerves are regenerated through 100 μm hole diameters do they recover anatomically more or less normal, after 4 to 16 weeks of regeneration, but with about 40% loss of force in the corresponding muscle. Smaller holes yielded morphological and functional failures.

PLANAR MICRO ELECTRODE ARRAYS FOR CULTURED NEURONS

Planar microelectrode arrays, consisting of transparent leads (indium tin oxide, or gold) to between 10 and 100 electrode sites (diameter typically 10 μm), spaced at 100 μm interdistance on glass plates, were used by Gross et al. (44,45), Novak and Wheeler (46), and others to study the activity and plasticity of developing cultured neuronal networks or brain slices. In this way, an attractive alternative was sought for the almost impossible job of probing many neurons in a growing network by micropipettes.

An essential prerequisite for high-quality recordings is to lower the high impedance of the tiny electrode sites to below about 1 MΩ by additional electroplating of Pt-black (47) and to increase the sealing resistance between cell and substrate by promoting adhesion. The latter can be achieved by coating of the glass substrate with laminin-, polylysine-, or silane-based (mono)layers (48–50).

Yet a number of neurons will adhere too far away from the electrode sites to produce measurable action potentials. This led Tatic-Lucic et al. (51) to the design of arrays consisting of electrode wells, in which single embryonic neural somata were locked up. Only their neurites could protrude from the well to form neural networks. In this way, unique contacts are established, to be used as bidirectional probes into the network. Alternatively, one can improve the contact efficiency by patterning the adhesive layer; it is even possible to guide neural growth (52); for example, around and over electrodes. On the electrode side, improvements are sought by incorporating an insulated gate field effect transistor (ISFET) in each electrode (53).

There is a considerable difference regarding whether stimulation or recording concerns an axon in a peripheral nerve

trunk or a nerve cell body (called soma) lying over an electrode site on a multielectrode substrate. This is studied by modeling and measurement of electrode impedance as a function of cell coverage and adhesion (54–56).

Except for neural network studies, cultured arrays may once be used as cultured neuron probes. They may be implanted in living nerve tissue to serve as a hybrid interface between electronics and nerve. The advantage would be that the electrode–cell interface may be established and optimized in the lab, while the nerve network after implantation may be a realistic target for ingrowth of nerve (collaterals). Studies of the feasibility of this approach are currently underway.

CHRONIC IMPLANTATION AND BIOCOMPATIBILITY

For future use in humans, chronic implantation behavior and biocompatibility studies of microelectrode arrays will become of crucial importance.

McCreery et al. (57) implanted single Ir microwire electrodes in cat cochlear nucleus and found tissue damage after long stimulation, highly correlated to the amount of charge per phase. The safe threshold was 3 nC/phase (while the stimulus threshold was about 1 nC/phase). Lefurge et al. (32) implanted intrafascicularly Teflon-coated Pt–Ir wires, diameter 25 μm. They appeared to be tolerated well by cat nerve tissue for six months, causing little damage. The influence of silicon materials silicon microshaft array rabbit and cat cortical tissue was investigated by Edell et al. (58) and Schmidt et al. (59). While neuron density around the 40 μm shafts decreased, tissue response along the shafts was minimal over six months (58), except at the sharp tips.

BIBLIOGRAPHY

1. D. McNeal, Analysis of a model for excitation of myelinated nerve, *IEEE Trans. Biomed. Eng.,* **23**: 329–337, 1976.
2. F. Rattay, Analysis of models for extracellular fiber stimulation, *IEEE Trans. Biomed. Eng.,* **36**: 676–683, 1989.
3. E. Warman, W. M. Grill, and D. Durand, Modeling the effect of electric fields on nerve fibers: Determination of excitation threshold, *IEEE Trans. Biomed. Eng.,* **39**: 1244–1254, 1992.
4. S. Nagarajan and D. Durand, Effects of induced electric fields on finite neuronal structures: A simulation study, *IEEE Trans. Biomed. Eng.,* **40**: 1175–1188, 1993.
5. W. M. Grill, Jr. and J. T. Mortimer, The effect of stimulus pulse duration on selectivity of neural stimulation, *IEEE Trans. Biomed. Eng.,* **43**: 161–166, 1996.
6. J. H. Meier et al., Simulation of multipolar fiber selective neural stimulation using intrafascicular electrodes, *IEEE Trans. Biomed. Eng.,* **39**: 122–134, 1992.
7. J. H. Meier, W. L. C. Rutten, and H. B. K. Boom, Force recruitment during electrical nerve stimulation with multipolar intrafascicular electrodes, *Med. Biol. Eng. Comput.,* **33** (3): 409–417, 1995.
8. P. H. Veltink et al., A modeling study of nerve fascicle stimulation, *IEEE Trans. Biomed. Eng.,* **36**: 683–692, 1989.
9. E. V. Goodall et al., Modeling study of size selective activation of peripheral nerve fibers with a tripolar cuff electrode, *IEEE Trans. Rehabil. Eng.,* **3**: 272–282, 1995.
10. W. L. C. Rutten, H. van Wier, and J. M. H. Put, Sensitivity and selectivity of intraneural stimulation using a silicon electrode array, *IEEE Trans. Biomed. Eng.,* **38**: 192–198, 1991.
11. W. L. C. Rutten, J. P. A. Smit, and J. A. Bielen, Two-dimensional neuro-electronic interface devices: Force recruitment, selectivity and efficiency, *Cell. Eng.,* **2** (4): 132–137, 1997.
12. W. L. C. Rutten et al., 3-D Neuro-electronic interface devices for neuromuscular control: Design studies and realisation steps, *Biosensors Bioelectron.,* **10**: 141–153, 1995.
13. K. L. Drake et al., Performance of planar multisite microprobes in recording extracellular single-unit intracortical activity, *IEEE Trans. Biomed. Eng.,* **35**: 719–732, 1988.
14. D. A. Evans et al., Multiple-channel stimulation of the cochlear nucleus, *Otolaryngol. Head Neck Surg.,* **101**: 651–657, 1989.
15. D. J. Anderson et al., Batch-fabricated thin-film electrodes for stimulation of the central auditory system, *IEEE Trans. Biomed. Eng.,* **36**: 693–704, 1989.
16. S. J. Tanghe, K. Najafi, and K. D. Wise, A planar IrO multichannel stimulating electrode for use in neural prostheses, *Sensors Actuators,* **B1**: 464–467, 1990.
17. J. Ji, K. Najafi, and K. D. Wise, A scaled electronically-configurable multichannel recording array, *Sensors Actuators,* **A22**: 589–591, 1990.
18. J. Ji and K. D. Wise, An implantable CMOS circuit interface for multiplexed microelectrode recording arrays, *IEEE J. Solid-State Circuits,* **26**: 433–443, 1992.
19. S. J. Tanghe and K. D. Wise, a 16-channel CMOS neural stimulating array, *IEEE J. Solid-State Circuits,* **27**: 1819–1825, 1992.
20. A. C. Hoogerwerf and K. D. Wise, A 3D micro-electrode array for chronic neural recording, *IEEE Trans. Biomed. Eng.,* **41**: 1136–1146, 1994.
21. C. Kim and K. D. Wise, A 64-site multishank CMOS low-profile neural stimulating probe, *IEEE J. Solid-State Circuits,* **31**: 1230–1238, 1996.
22. D. T. Kewley et al., Plasma-etched neural probes, *Sensors Actuators,* **A58**: 27–35, 1997.
23. K. Najafi, J. Ji, and K. D. Wise, Scaling limitations of silicon multichannel recording probes, *IEEE Trans. Biomed. Eng.,* **37**: 1–11, 1990.
24. K. Najafi and J. F. Hetke, Strength characterization of silicon microprobes in neurophysiological tissues, *IEEE Trans. Biomed. Eng.,* **37**: 474–481, 1990.
25. J. F. Hetke, K. Najafi, and K. D. Wise, Flexible miniature ribbon cables for long-term connection to implantable sensors, *Sensors Actuators,* **A23**: 999–1002, 1990.
26. J. F. Hetke et al., Silicon ribbon cables for chronically implantable microelectrodes arrays, *IEEE Trans. Biomed. Eng.,* **41**: 314–321, 1994.
27. P. K. Campbell et al., A silicon-based three-dimensional neural interface: Manufacturing processes for an intracortical electrode array, *IEEE Trans. Biomed. Eng.,* **38**: 758–768, 1991.
28. C. T. Nordhausen, P. J. Rousche, and R. A. Normann, Optimizing recording capabilities of the Utah intracortical electrode array, *Brain Res.,* **637**: 27–36, 1994.
29. W. Ehrfeld and D. Munchmeyer, LIGA method, three dimensional microfabrication using synchrotron radiation, *Nucl. Instrum. Methods Phys. Res.,* **A303**: 523–531, 1991.
30. J. T. Mortimer et al., Perspectives on new electrode technology for stimulating peripheral nerves with implantable motor prostheses, *IEEE Trans. Rehabil. Eng.,* **3**: 145–154, 1995.
31. M. Malagodi, K. W. Horch, and A. A. Schoenberg, An intrafascicular electrode for recording of action potentials in peripheral nerves, *Ann. Biomed. Eng.,* **17**: 397–410, 1989.
32. T. Lefurge et al., Chronically implanted intrafascicular recording electrodes, *Ann. Biomed. Eng.,* **19**: 197–207, 1991.
33. N. Nannini and K. Horch, Muscle recruitment with intrafascicular electrodes, *IEEE Trans. Biomed. Eng.,* **38**: 769–776, 1991.

34. E. V. Goodall and K. W. Horch, Separation of action potentials in multi-unit intrafascicular recordings, *IEEE Trans. Biomed. Eng.,* **39**: 289–295, 1992.
35. T. McNaughton and K. Horch, Action potential classification with dual channel intrafascicular electrodes, *IEEE Trans. Biomed. Eng.,* **41**: 609–616, 1994.
36. T. G. McNaughton and K. W. Horch, Metallized polymer fibers as leadwires and intrafascicular microelectrodes, *J. Neurosci. Methods,* **70**: 103–110, 1996.
37. K. Yoshida and K. Horch, Reduced fatigue in electrically stimulated muscle using dual channel intrafascicular electrodes with interleaved stimulation, *Ann. Biomed. Eng.,* **21**: 709–714, 1993.
38. K. Yoshida and K. Horch, Closed-loop control of ankle position using muscle afferent feedback with functional neuromuscular stimulation, *IEEE Trans. Biomed. Eng.,* **43**: 167–176, 1996.
39. D. J. Edell, A peripheral nerve information transducer for amputees: Long-term multichannel recordings from rabbit peripheral nerves, *IEEE Trans. Biomed. Eng.,* **33**: 203–214, 1986.
40. G. T. A. Kovacs, C. W. Storment, and J. M. Rosen, Regeneration microelectrode array for peripheral nerve recording and stimulation, *IEEE Trans. Biomed. Eng.,* **39**: 893–902, 1992.
41. G. T. A. Kovacs et al., Silicon-substrate micro-electrode arrays for parallel recording of neural activity in peripheral and cranial nerves, *IEEE Trans. Biomed. Eng.,* **41**: 567–577, 1994.
42. Q. Zhao et al., Rat sciatic nerve regeneration through a micromachined silicon chip, *J. Biomater.,* **18**: 75–80, 1997.
43. A. Blau et al., Characterization and optimization of microelectrode arrays for in-vivo nerve signal recording and stimulation, *Biosensors Bioelectron.,* **12**: 883–892, 1997.
44. G. W. Gross, Simultaneous single unit recording in vitro with a photoetched laser deinsulated gold multimicroelectrode surface, *IEEE Trans. Biomed. Eng.,* **26**: 273–279, 1979.
45. G. W. Gross, W. Y. Wen, and J. W. Lin, Transparent indium-tin oxide electrode patterns for extracellular, multisite recording in neuronal cultures, *J. Neurosci. Methods,* **15**: 243–252, 1985.
46. J. L. Novak and B. C. Wheeler, Recording from the Aplysia abdominal ganglion with a planar microelectrode array, *IEEE Trans. Biomed. Eng.,* **33**: 196–202, 1986.
47. W. Nisch et al., A thin film microelectrode array for monitoring extracellular neuronal activity in vitro, *Biosensors Bioelectron.,* **9**: 737–741, 1994.
48. J. P. Ranieri et al., Spatial control of neuronal cell attachment and differentiation on covalently patterned laminin oligopeptide substrates, *Int. J. Develop. Neurosci.,* **12** (8): 725–735, 1994.
49. J. F. Clemence et al., Photoimmobilization of a bioactive laminin fragment and pattern-guided selective neuronal cell attachment, *Bioconjugate Chem.,* **6** (4): 411–417, 1995.
50. J. M. Corey, B. C. Wheeler, and G. J. Brewer, Micrometer resolution silane-based patterning of hippocampal neurons: A comparison of photoresist and laser ablation methods of fabricating substrates, *IEEE Trans. Biomed. Eng.,* **43**: 944–955, 1996.
51. S. Tatic-Lucic et al., Silicon-micromachined neurochips for in vitro studies of cultured neural networks, *Proc. 7th Int. Conf. Solid State Sensors Actuators,* Yokohama, Japan, 1993, pp. 943–946.
52. D. W. Branch et al., Microstamp patterns of biomolecules for high-resolution neuronal networks, *Med Biol. Eng. Comput.,* **36**: 135–141, 1998.
53. A. Stett, B. Muller, and P. Fromherz, Two-way silicon-neuron interface by electrical induction, *Phys. Rev. E,* **55**: 1779–1782, 1997.
54. R. Weis and P. Fromherz, Frequency dependent signal transfer in neuron transistors, *Phys. Rev. E,* **55**: 877–889, 1997.
55. M. Bove, M. Grattarola, and G. Verreschi, In vitro 2-D networks of neurons characterized by processing the signals recorded with a planar microtransducer array, *IEEE Trans. Biomed. Eng.,* **44** (10): 964–978, 1997.
56. J. R. Buitenweg et al., Measurement of sealing resistance of cell-electrode interfaces in neuronal cultures using impedance spectroscopy, *Med. Biol. Eng. Comput.,* 1998.
57. D. B. McCreery et al., Stimulus parameters affecting issue injury during microstimulation in the cochlear nucleaus of the cat, *Hear. Res.,* **77**: 105–115, 1994.
58. D. J. Edell et al., Factors influencing the biocompatibility of insertable silicon microshafts in cerebral cortex, *IEEE Trans. Biomed. Eng.,* **39**: 635–643, 1992.
59. S. Schmidt, K. Horch, and R. Normann, Biocompatibility of silicon-based electrode arrays implanted in feline cortical tissue, *J. Biomed. Mater. Res.,* **27**: 1393–1399, 1993.
60. D. A. Stenger and T. M. McKenna (eds.), *Enabling Technologies for Cultured Neural Networks,* San Diego, CA: Academic Press, 1994.

Reading List

I. A. Boyd and M. R. Davey, *Composition of Peripheral Nerves,* Edinburgh: Livingstone, 1968.
W. F. Agnew and D. B. McCreery (eds.), *Neural Prostheses Fundamental Studies,* Englewood Cliffs, NJ: Prentice-Hall, 1990.
J. Malmivuo and R. Plonsey, *Bioelectromagnetism,* Oxford, UK: Oxford Univ. Press, 1995.

WIM L. C. RUTTEN
University of Twente

NEUTRON FLUX MEASUREMENT. See FISSION CHAMBERS.

NIGHT PILOTAGE, HELICOPTER. See HELICOPTER NIGHT PILOTAGE.

NMR. See MAGNETIC RESONANCE.